Computer Methods in Biomechanics and Biomedical Engineering, Vol. 00, pp. 1–15
Reprints available directly from the publisher
Photocopying permitted by license only

Finite-element Analysis of a Stenotic Artery Revascularization through a Stent Insertion

F. AURICCHIO[a,*], M. DI LORETO[b] and E. SACCO[c]

[a]*Dipartimento di Meccanica Strutturale, Università di Pavia, Italy;* [b]*Dipartimento di Ingegneria Civile, Università di Roma "Tor Vergata", Italy;* [c]*Dipartimento di Meccanica, Strutture, A.&T., Università di Cassino, Italy*

(Received in final form 20 May 2000)

Short-term and long-term clinical follow-up data clearly indicate the superiority of stenting techniques within the family of mechanical treatments for percutaneous coronary revascularizations. However, restenosis phenomena are in general still present, representing the major drawback for this innovative non-invasive approach.

Experimental evidence indicates the mechanical interaction between the stent and the artery as a significant cause for the activation of stent-related restenosis. At the same time, the literature shows a significant lack of computational investigations within this field, possibly as consequence of the complexity of the problem.

According to these considerations, the aim of the present work is to study the bio-mechanical interaction between a balloon-expandable stent and a stenotic artery, highlighting considerations able to improve the general understanding of the problem.

In particular, given an initial stent design (J&J Palmaz-Schatz like), we show the presence of possible areas of artery injury during the stent deployment and areas of non-uniform contact pressure after the stent apposition, due to a non-uniform stent expansion. Since these concentrated mechanical actions can play an important role in the activation of restenosis mechanisms, we propose a modified stent design, which shows a more uniform expansion and for which typical stenting parameters (*i.e.*, residual stenosis, elastic recoil, foreshortening) are computed and presented.

Keywords: Balloon-expandable stent; Stent apposition; Revascularization; Finite-element; Large deformation analysis; Contact pressure

*Corresponding author. Dipartimento di Meccanica Strutturale, Università di Pavia, *Via* Ferrata 1, 27100 Pavia, Italy. e-mail: auricchio@unipv.it

1. INTRODUCTION

Cardiac diseases represent the most common cause of death in Western countries and they are often related to coronary atherosclerosis [1], *i.e.*, to deposits and fibrosis of the artery inner layer producing a local lumen narrowing or occlusion, in general indicated as stenosis.

While such artery pathologies have been traditionally treated through either pharmacological therapies or invasive surgeries (such as by-passes), recently, non-invasive approaches are more and more often preferred.

Non-invasive treatments are in general based on the insertion of a guide-wire in the vascular system through a peripheral artery (such as the femoral or the brachial one) and on the subsequent use of a catheter, whose tip is equipped with a mechanical device, used to remove the occlusion.

Due to the less traumatic nature, non-invasive techniques usually result in shorter hospital stays as well as in reduced post-intervention complications. On the other hand, they may produce long-term re-occlusion phenomena (restenosis), requiring sometimes a successive revascularization [1].

Classical examples of non-invasive treatments are the PTCA and the stenting techniques. The PTCA (Percutaneous Transluminal Coronary Angioplasty) uses a balloon as a mechanical device to re-open the occluded artery, while the stenting technique is based on the insertion of a permanent tubular structure (stent) at the lesion site. In general, the stent has also the roles of supporting the arterial walls, after the catheter retrieval (Fig. 1).

Compared to the PTCA, the stent induces an even greater increment in intervention effectivenesses and in success rates [1]. These considerations justify the high interest that both the commercial and the scientific communities are showing toward the stent technique.

However, a search on well-established databases has highlighted a considerable research effort devoted to the investigation of typical medical aspects related to the stenting technique, such as material bio-compatibilities, thrombosis and neointimal pathologies. On the other hand, bio-mechanical studies have received much more limited attention. This observation is even more surprising since available experimental studies clearly indicate the stent-artery mechanical interaction as one of the significative causes for the activation of restenosis mechanisms [1–3]. In an attempt to partially justify such disomogeneities in scientific efforts, it should be pointed out the complexity of performing an accurate bio-mechanical modeling for a stenting intervention. In fact, besides the usual difficulties in modeling the mechanical behavior of soft tissues, the overall system response is highly non-linear, due to the large deformations of the single components – that is, stent, plaque and artery – and to their interaction.

Accordingly, the present work is directed toward a better understanding of coronary stenting bio-mechanics. In particular, the paper is organized as follows. Section 2 presents an overview of the stenting technique, together with a review on the state of the art of stenting bio-mechanical studies. Section 3 describes a three-dimensional model for the revascularization of a stenotic artery through the insertion of a balloon-expandable stent, briefly commenting also on the state of the art relative to soft tissue constitutive modeling. Section 4 discusses results obtained from the large-deformation analysis of the model presented, focusing the attention on two different stent designs and investigating their relative ability to induce an effective revascularization. Finally, Section 5 draws some conclusions and directions for future work.

2. THE STENTING METHODOLOGY

We now present a brief overview on the stenting technique, reporting procedural and follow-up results from the literature and highlighting the absence of accurate bio-mechanical investigations.

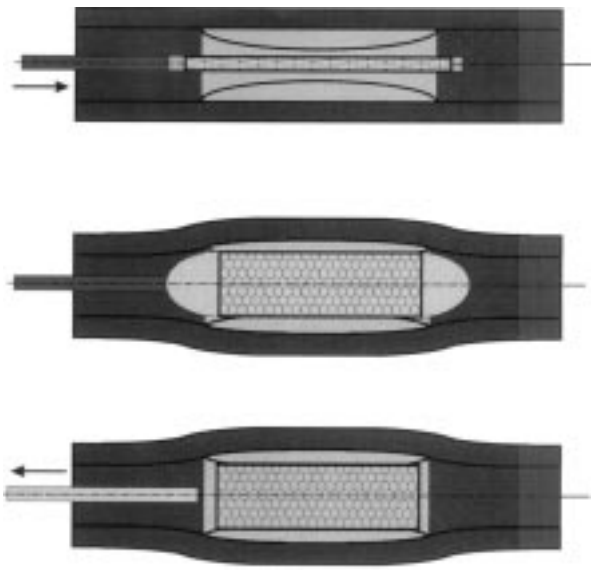

FIGURE 1 Schematic representation of apposition phases for a balloon-expandable stent. The figure shows: (1) the placement of the delivery system at the lesion site; (2) the inflation of the balloon with the apposition of the stent; (3) the removal of the delivery system. In general, the stent has the role of supporting the arterial wall also after the catheter retrieval.

2.1. Stenting Outcomes and Bio-medical Considerations

Initially introduced in 1964 by Dotter and Judkins [4], the stenting methodology is based on the implant of a tubular endoprosthesis (stent) to support the arterial wall. In general, the stent is mounted on the tip of a catheter (also indicated as delivery system); once at the lesion site, the stent is released from the delivery system to expand and support the arterial wall.

Regularly employed since the end of the 80's, stents can be considered as the most important advance in mechanical techniques for percutaneous coronary revascularizations [1, 5] and this explains the related proliferative activities both in the commercial and in the scientific community.

As an example of the current methodology sophistication, we may distinguish at least three different approaches, simply based on the expansion mechanism: balloon-expandable, self-expandable and thermally expandable stents [1, 6]. In the following we limit our attention only to balloon-expandable stents, being the most frequently adopted.

The balloon-expandable stents are in general made of a metallic alloy (such as stainless steel, tantalum, *etc*.) and they take advantage of the material plastic properties. In fact, once positioned at the lesion site, the stent is plastically expanded by a PTCA-like balloon. After the balloon deflation and retrieval, apart from a small elastic recoil the stent continues to support the arterial wall (Fig. 1).

In the last two decades, several randomized and observational studies have compared immediate and long-term results (1 year) of stenting *versus* PTCA [1, 7–13]. According to these investigations, stenting can be performed with a high procedural success ($>90\%$) and a low complication rate ($<5\%$), as the PTCA. However, the PTCA results in a residual stenosis of $\approx 30\%$, a restenosis of $40-50\%$ and a restenosis rate of 40%, while stenting results in a residual stenosis $<5\%$, a restenosis $<30\%$ and a restenosis rate of $\approx 20\%$. Finally, the need for target lesion revas-

cularizations is in general of the order of 21% with the PTCA compared to the 10% with the stent.

The favorable impact of stenting on restenosis relates to its ability to achieve a superior and smoother lumen enlargement, to minimize the artery elastic recoil and to virtually eliminate the arterial remodeling. Hence, even if a stent may induce a major intimal thickening with respect to PTCA, this is more than offset by its other beneficial effects.

However, compared to the PTCA, the stent induces more complex and varied restenosis mechanisms.

In fact, on one hand the stent is a permanent implant, introducing all the aspects related to the material biocompatibility and to thrombo-genesis mechanisms. To limit these problems, researchers are progressively improving the bulk material biocompatibility (for example through chemical and thermal treatments), introducing new production technologies (such as laser cutting) or specific surface treatments (such as electro-polishing, drug or radio-active coatings).

On the other hand, the stent exerts local actions on the artery, actions which clearly depend on the specific design as well as on the implant technique [2]. In particular, during the deployment and the apposition the stent may induce vascular injuries and even dissections, which can clearly be major causes of restenosis mechanisms. Accordingly, there exists a large area of possible research directed toward a minimization of these injuries and based on the optimization of stent designs (such as stent-strut geometries) and of stent placement protocols (such as balloon and inflation pressure selections) [1, 3, 5, 6].

2.2. State of the Art on Bio-mechanical Studies

Despite the need for accurate mechanical studies on the stent technique in general and on the stent-artery interaction, these areas of research have received very limited attention. In the following we briefly review some studies available in the literature.

Perry and Chang simulate the deployment of a self-expandable stent considering the interaction with a rigid atherosclerosis plaque [14]. The lesion is assumed to have a constant longitudinal profile and an asymmetrical cross-section profile. The problem is studied considering only a single strut, *i.e.*, a single longitudinal modulus.

Auricchio and Taylor study the deployment of a self-expandable stent [15]. Taking advantage of the problem symmetry, the simulation is relative to a single strut. Particular attention is devoted to the stent material constitutive behavior, while no interaction with an atherosclerosis plaque is considered.

Whitcher investigates the fatigue resistance of a self-expandable stent subject to systolic/diastolic cycles [16]. Again, due to symmetry considerations, only a single strut is considered. The artery action on the stent is modeled as a uniform pressure and only two pressure values are considered to reproduce the systole and the diastole conditions, respectively.

Trochu and Terriault simulate a stent deployment into a rigid vessel, comparing stainless steel and self-expandable stents [17, 18]. The attention is again focused on a single strut, modeled with beam elements.

Rogers *et al.*, concentrate on the balloon/artery interaction between stent struts during the stent apposition phase [19]. The aim is to provide a better understanding of endothelial denudation mechanisms induced by the balloon expansion. A two-dimensional cross-sectional model is developed but the researchers did not consider the stent apposition phase and neglected the presence of plaque; moreover, both the artery and the balloon are assumed to behave as linearly elastic.

For completeness, we also report some experimental *in-vitro* investigations, such as the work by Andrews *et al.*, relative to the stent fixation inside the artery [20] and the work by Glenn *et al.*, focused on the fatigue-life of a stent subject to systolic/diastolic loading cycles [21].

During the bibliographic search, we also found other interesting References, relative to the non-invasive interventistic surgery, and, hence, related to the present research. As an example, we recall the work of Holzapfel *et al.*, who concentrate on the PTCA technique [22].

2.2.1. A Final Remark

We wish to conclude the Section paraphrasing the "New Manual of Interventional Cardiology": stents are the most important advance in mechanical techniques for percutaneous coronary revascularization and it is quite likely that this revolutionary technology may ultimately account for $> 50\%$ of all percutaneous interventions ([1] p. 505).

However, the bio-mechanical analysis of stenting techniques is a field still requiring attention. This consideration is particularly true due to the fact that most of the studies available in the literature neglect some – or all – the following aspects:

- the system is composed of three elements – stent, plaque and artery – and the interaction between the single components plays a non-negligible role,
- the three components have different and somehow quite complex constitutive behavior,
- the investigated problem is in general fully three-dimensional.

3. MODELING OF A STENOTIC ARTERY REVASCULARIZATION THROUGH A STENT INSERTION

To investigate the revascularization of a stenotic artery through the insertion of a balloon-expandable stent, we develop a three-dimensional model of the complete system, *i.e.*, stent, plaque and artery. A large-deformation analysis is then performed using the commercial finite-element code Abaqus (MK&S) [23] and numerical results are discussed in Section 4.

3.1. Model Geometry

We consider a straight artery segment with a length of 26 mm and a lumen diameter of 3 mm (Fig. 2). The artery thickness is set equal to 1/4 of the lumen (0.75 mm), following typical coronary proportions.

The plaque has a parabolic longitudinal profile and it is symmetrically positioned within the cross section ("symmetric stenosis"). The plaque has a longitudinal length of 13 mm, with a maximum thickness of 0.7 mm; accordingly, it reduces the artery lumen from the original 3 mm to 1.6 mm, reproducing a 53% stenosis (a typical value after PTCA pre-treatment [1]).

In the unexpanded configuration the stent is assumed to be a tube with rectangular slots along its length (Fig. 3). Its initial length, inner and outer diameters are respectively equal to 16 mm, 1 mm and 1.2 mm. The stent has 5 slots in the longitudinal direction and 12 slots in the circumferential direction, each slot measuring 2.88 mm times 0.24 mm.

Due to symmetry considerations, we consider only half of a 30° three-dimensional segment of the whole model (Fig. 4).

3.2. Constitutive Equations

We now discuss the constitutive equations adopted in the present work to describe the behavior of the system single components.

3.2.1. Artery and Plaque

A large amount of experimental data on the mechanical properties of vascular tissue is available in the literature. However, general indications are quite difficult to extract, due to the low standardization of the experimental settings, the great variety of tissue typologies as well as the

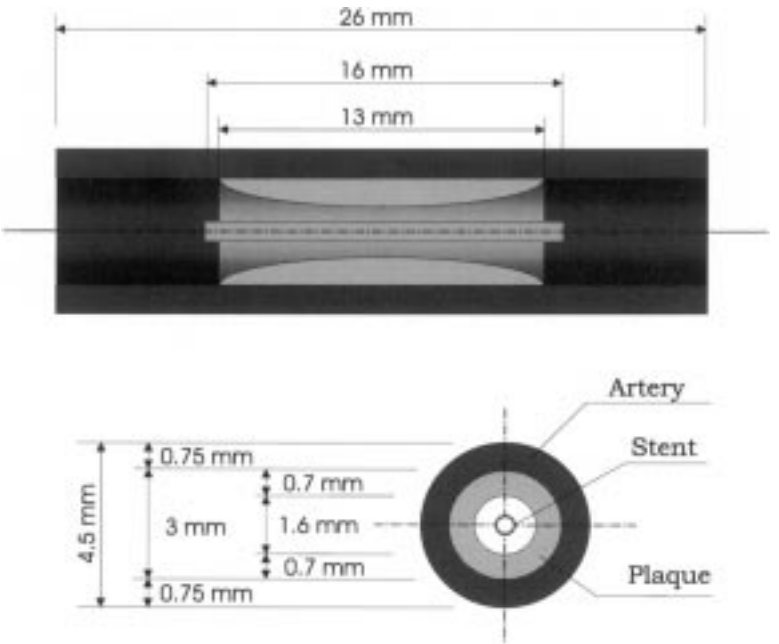

FIGURE 2 Pictorial description of the complete system (stent, artery, plaque) before the stent apposition and indications on the dimensions of the considered model.

FIGURE 3 Original stent design: unexpanded configuration. The stent is assumed to be a tube of length, inner and outer diameters respectively equal to 16 mm, 1 mm and 1.2 mm. The tube has 5 rectangular slots in the longitudinal direction and 12 slots in the circumferential direction, each slot measuring 2.88 mm times 0.24 mm.

complex artery anatomic structure. These aspects are even more delicate when applied to diseased vessels – such as stenotic lumens –, also as a consequence of the large range of lesion typologies [24 – 27].

Due to the overall complexity, the constitutive modeling of arteries often requires significant approximations. As an example, the hysteretic behavior is often neglected, together with the smooth muscle cell contractile behavior, the residual strain presence and the remodeling process.

Moreover, arteries are often considered as homogeneous solids, sometimes assuming ortho-

FIGURE 4 Finite-element mesh considered during the analyses. Due to symmetry considerations, only half of a 30° three-dimensional segment of the whole model is considered in the analyses.

tropy along the artery axis and most of the time limiting the state of stress to a membranal one.[1]

The first models for arteries were developed in a small-deformation setting, considering vascular tissues as linear elastic materials and in some cases taking into account their non-isotropic properties [30, 31].

In the late 80's, two- and three-dimensional models were developed, in an attempt to better describe the artery behavior (for example in the large deformation range). Based on the hyperelasticity theory [32], these models introduce an strain energy function U in term of a finite strain deformation measure, in most cases the Green–Lagrange tensor. Four main strain energy functions have been discussed in the literature: polynomial, exponential, logarithmic and polynomial–exponential ones.

The polynomial functions were the first to be proposed and they have the drawback of requiring a large number of material constants to properly fit experimental data [33, 34]. Exponential and logarithmic forms require fewer material constants, showing a good fitting ability especially in the large deformation regime [33, 35].

Finally, polynomial–exponential forms allow a good fit of experimental data in both the small and the large deformation regimes with fewer material constants [22, 36, 37]. As an example, Holzapfel and Weizsäcker recently proposed to combine an isotropic polynomial term with an orthotropic exponential term, with the idea that the first term could describe the elastic mechanical contribution, while the second one could take into account the collagen contribution [38].

Our Approach We follow the data obtained by Hayashi and Yosuke [24] and relative to a stenotic rabbit aorta in the passive state. In particular, starting from soft atherosclerotic artery segments, Hayashi and Yosuke dissect the plaque from the artery, testing separately the two tissues in a uniaxial state and reporting the results for a wide range of deformations.

The adopted approach seems to properly address the response of the single constituents – plaque and artery –, in particular taking into account the influence of the plaque formation on the artery mechanical properties. On the other

[1] Fung *et al.*, studied a two-layered model (intima-media and adventitia), considering each layer as linearly elastic and in a small deformation range [28]. Finally, Von Maltzahn *et al.*, considered also the non-linear behavior of the layers [29].

hand, it neglects the artery laminate compositions as well as the tissue anisotropy. Due to the limitation of data available (only one-dimensional test), in our investigations we consider the artery and the plaque as homogeneous isotropic materials. [2] Moreover, we neglect the residual strain and the remodeling effects; finally, we consider the assumption of incompressibility to be valid which is the classical position in the bio-mechanics of soft tissue.

Accordingly, we point our attention toward three-dimensional hyperelastic isotropic incompressible models. This choice is somehow different from what is usually referenced in the literature, where arteries are mostly described as membranes. However, a three-dimensional approach is more accurate for the case of thick artery walls, and this will be investigated here.

Hyperelastic Isotropic Models The constitutive response of an hyperelastic isotropic material is described introducing a strain energy U, function of the left Cauchy–Green tensor $\mathbf{B}$ through its invariants [32]. Recalling that $\mathbf{B}=\mathbf{F}\mathbf{F}^T$ with $\mathbf{F}$ being the deformation gradient, we set:

$$U = U(I_1, I_2, J) \tag{1}$$

where

$$I_1 = \mathrm{tr}(\mathbf{B}) = (\lambda_1)^2 + (\lambda_2)^2 + (\lambda_3)^2 \tag{2}$$

$$I_2 = \mathrm{tr}[\mathrm{adj}(\mathbf{B})] = \lambda_1\lambda_2 + \lambda_1\lambda_3 + \lambda_2\lambda_3 \tag{3}$$

$$J = \det(\mathbf{F}) = \lambda_1\lambda_2\lambda_3 \tag{4}$$

with $\lambda_i (i=1,2,3)$ the principal stretches of $\mathbf{F}$.

In particular, we choose the following polynomial strain energy:

$$U = \sum_{i+j=1}^{N} [C_{ij}(I_1-1)^i(I_2-1)^j] + \hat{p}(J-1) \tag{5}$$

where C_{ij} are material constants and $\hat{p}$ is the Lagrange multiplier enforcing the incompressibility constraint $J=1$. According to Eq. (1), the Cauchy stress $\boldsymbol{\sigma}$ is given by:

$$\boldsymbol{\sigma} = \hat{p}\mathbf{1} + 2\left[\left(\frac{\partial U}{\partial I_1} + I_1\frac{\partial U}{\partial I_2}\right)\mathbf{B} - \frac{\partial U}{\partial I_2}\mathbf{B}^2\right] \tag{6}$$

where $\mathbf{1}$ is the second-order identity tensor.

Experimental Data Fitting Using Eq. (6), we try to get a good fit of the experimental curves [24], attempting at the same time to reduce as much as possible the number of non-zero material constants, in order to improve the computational efficiency.

With this goal in mind, for the artery and the plaque we choose the material constants C_{ij} reported in Table I. Figure 5 shows a comparison between the experimental data and the model response in terms of uniaxial Cauchy stress (σ) *versus* uniaxial stretch (λ).

The results of Figure 5 and of Table I are of particular interest, especially considering that in general polynomial strain energy functions are discarded in consideration of the high number of terms which should be introduced to get an adequate match with experimental data. For the case investigated here, we are able to get an excellent match with a very limited number of non-zero material constants: three for the plaque (C_{10}, C_{02}, C_{03}) and two for the artery (C_{10}, C_{03}).

It is also interesting to note that the good match between the model response and the experimental data can be interpreted, following the work of Holzapfel and Weizsäcker [38]. Limiting for

TABLE I Material constants for the artery and the plaque

Constant	Artery	Plaque
C_{10}	19513 MPa	2176 MPa
C_{01}	0 MPa	1480 MPa
C_{03}	29760 MPa	13431 MPa

[2] This is clearly a limiting and somehow unrealistic assumption due to the lack of accurate experimental data. More realistic and appropriate assumptions can be introduced only in the presence of a more detailed set of experimental data.

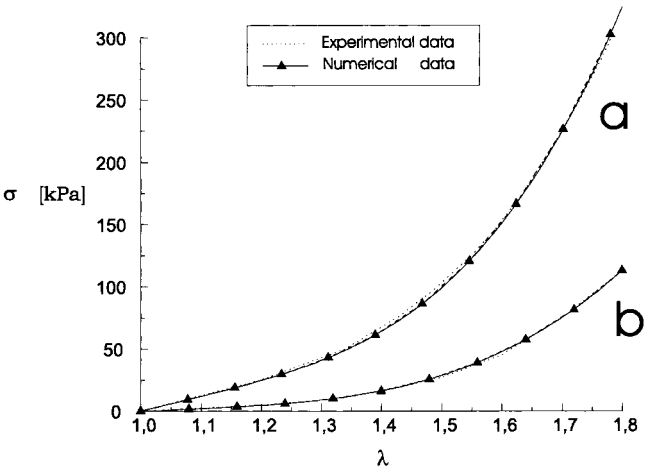

FIGURE 5 Comparison between the experimental data [24] and the model response (numerical data) for the artery (curve a) and the plaque (curve b).

example the discussion to the artery, we may associate the C_{10} and C_{03} terms to specific artery components.

In fact, the C_{10} term gives the classical Neo-Hookean response, able to reproduce the nearly linear behavior of the elastic structures present in the artery wall, while the C_{03} term should take into account the behavior of the other artery components. However, since Hayashi's experimental data refer to *ex-vivo* aortas in the passive state, the influence of smooth muscle cells is negligible and we can refer the C_{03} term to the collagen structures alone.

3.2.2. Stent

The stent is assumed to be made of SS316LN stainless steel, similar to the SS316L steel used in many commercial balloon-expandable stents, such as the original J&J Palmaz-Schatz. The SS316LN inelastic constitutive response is described through a Von Mises–Hill plasticity model with isotropic hardening [39].

The model is based on a multiplicative split of the deformation gradient $\mathbf{F}$ into an elastic part, $\mathbf{F}^{el}$, and a plastic part, $\mathbf{F}^{pl}$ [40–42]:

$$\mathbf{F} = \mathbf{F}^{el}\mathbf{F}^{pl} \tag{7}$$

Introducing the total, elastic and plastic velocity gradients, defined respectively as:

$$\mathbf{L} = \dot{\mathbf{L}}(\mathbf{F})^{-1}, \quad \mathbf{L}^{el} = \dot{\mathbf{L}}^{el}(\mathbf{F}^{el})^{-1}, \quad \mathbf{L}^{pl} = \dot{\mathbf{L}}^{pl}(\mathbf{F}^{pl})^{-1} \tag{8}$$

and the total, elastic and plastic strain rates defined as the symmetric parts of the corresponding velocity gradients:

$$\dot{\boldsymbol{\varepsilon}} = \mathrm{symm}(\mathbf{L}), \quad \dot{\boldsymbol{\varepsilon}}^{el} = \mathrm{symm}(\mathbf{L}^{el}), \quad \dot{\boldsymbol{\varepsilon}}^{pl} = \mathrm{symm}(\mathbf{L}^{pl}) \tag{9}$$

it is possible to prove that under the assumption of small elastic strains compared to the plastic strains, the following relation is valid:

$$\dot{\boldsymbol{\varepsilon}} = \dot{\boldsymbol{\varepsilon}}^{el} + \dot{\boldsymbol{\varepsilon}}^{pl} \tag{10}$$

The model adopted to describe the constitutive behavior of the stent is based on the extension of classical small deformation plasticity to the large deformation regime but expressed in terms of strain rates [23]. As examples, the elastic strain rate is related to the stress rate through a linear elastic

isotropic relation in terms of an elastic modulus E and a Poisson ratio ν, while the inelastic strain rate evolves following an associative flow rule:

$$\dot{\boldsymbol{\varepsilon}}^{\mathrm{pl}} = \dot{\gamma}\frac{\partial Y}{\partial \boldsymbol{\sigma}} \tag{11}$$

with γ the plastic consistency parameter and Y the yield criterium. As yield criterium, we choose a Von Mises – Hill function (*i.e.*, function only of the deviatoric part of the stress), combined with a piecewise linear hardening model. The piecewise linear hardening is described through a sequence of stress – strain couples, after yielding and up to a limit point, (*i.e.*, a stress – strain couple), indicated in the following as $\sigma_R - \epsilon_R$.

Table II reports the material constants adopted [43] while Figure 6 shows a comparison between the experimental data and the model response in terms of unixial Cauchy stress (σ) *versus* nominal strain ($\epsilon_{\mathrm{nom}} = \lambda - 1$). Again, excellent fitting between the two curves can be noted.

3.3. Loading Conditions, Finite Elements and Contact Conditions

Considering balloon-expandable stents, the stent apposition is induced through the inflation of a balloon. In general, the balloon is longitudinally longer than the stent and it is initially seated inside the stent. After the balloon inflation and the stent apposition, the balloon is deflated and removed.

From data available in the literature, we conclude that, compared to the stent, the balloon is a more flexible structural element. Accordingly, within an acceptable degree of approximation, it is reasonable to neglect the balloon stiffness compared to the stent stiffness. This position has a major consequence in permitting the possibility of discarding the presence of the balloon in the analysis, while at the same time considering the internal pressure of the balloon is directly applied to the stent.

TABLE II Material constants for the stent

Young modulus (E)	196000 MPa
Poisson ratio (ν)	0.3
Yield stress (σ_Y)	205 MPa
Limit stress (σ_R)	515 MPa
Limit nominal strain (ϵ_R)	60%

Hence, we load the stent by an internal uniform radial pressure. Following data present in literature, the pressure varies linearly from zero to 1.3 MPa (inflation) and then again linearly back to zero (deflation) [1, 5, 6].

Due to the artery incompressibility requirement and to avoid locking-problems, hybrid 8-node brick elements (C3D8H) are used in all the analyses [23]. In particular, in the simulations we use upto 3152 elements and 7849 nodes, resulting in 16883 variables.

Finally, the interaction between the expanding stent and the artery/plaque is described as contact between deformable surfaces. As contact conditions, we set finite sliding, no-friction, with the constraint enforced by a Lagrange multiplier method [23].

4. NUMERICAL RESULTS

We now present and discuss the results obtained from the large-deformation analysis of the model described in the previous section. From the analyses we are able to highlight some deficiencies of the initially adopted stent design and to propose an improved modified design.

4.1. Stent Free Expansion

We start by considering stent free expansion. This situation is clearly far from the one relative to the stent implant, when the interaction between the stent and the artery wall plays a significant role. However, the study of the free expansion makes possible on one hand to concentrate on the behavior of the stent alone and to show possible unexpected responses, on the other hand to highlight the configuration in which the stent

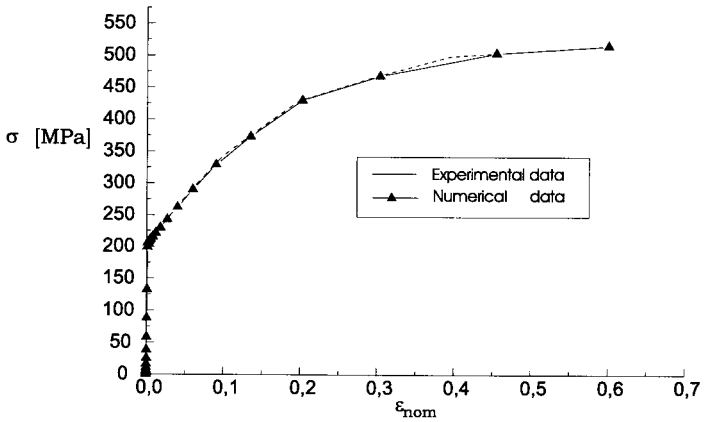

FIGURE 6 Comparison between the experimental data [43] and the model response (numerical data) for the stent.

enters into contact with the artery during the stent implant situation.

Figure 7 shows the results from the stent free expansion. It is interesting to observe how the stent does not present a uniform dilatation during the expansion. This highlights that during the stent implant the distal struts are the first to enter into contact with the artery and they may pinch the tissue, damaging it, activating local restenotic mechanisms and possibly producing dissections.

This problem can be overcome in various ways: it is possible for example to use shaped balloons, to change the stent design while keeping the radial thickness constant, or to adopt a variable radial thickness along the longitudinal direction of the stent.

We investigated the first two remedies, considering the last one to be too expensive from a stent manufacturing perspective. In particular, we found it difficult to correct the problem of changing the pressure distribution on the internal surface of the stent, while the possibility of changing the stent design seems very promising.

As an example, we consider a modified stent design, characterized by the presence of added distal struts (Fig. 8). The free-expansion of the modified stent is reported in Figure 9 and it is interesting to observe the uniform expansion now

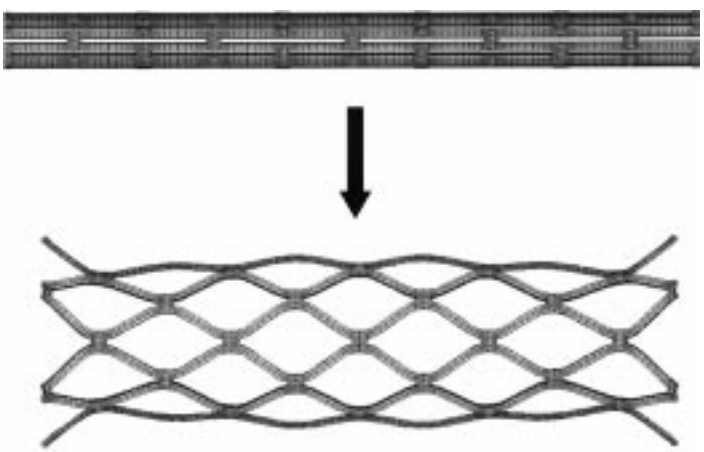

FIGURE 7 Original stent design: free expansion: It is interesting to observe the non uniform expansion.

FIGURE 8 Modified stent design: unexpanded configuration. It is possible to note the added distal struts.

example material resistance. However, this type of result is not reported here for brevity.

4.2. Revascularization of a Stenotic Artery

We now simulate the placement of the modified stent at a lesion site (balloon inflation) and the elastic recoil phase (balloon deflation). The goals are to verify the effective revascularization of the stenotic artery and to quantify the recoil. In particular, Figure 10 shows the final configuration of the stent and the artery after the balloon

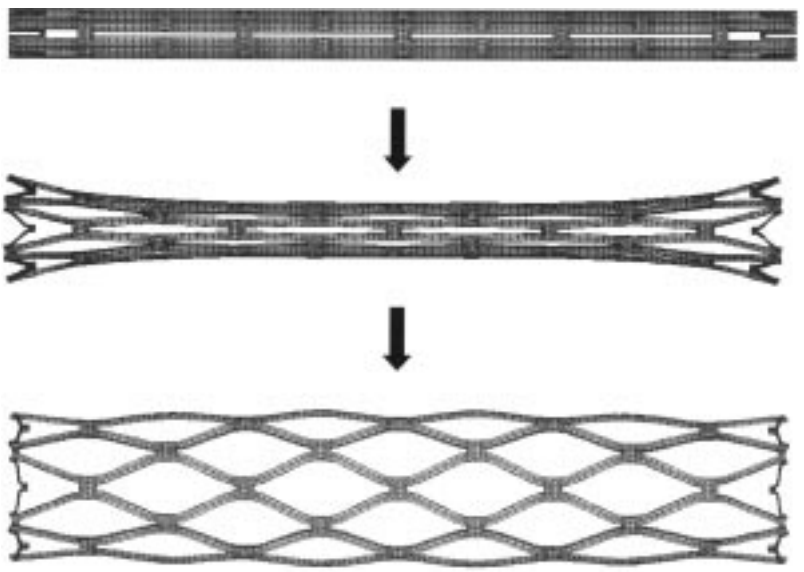

FIGURE 9 Modified stent design: free expansion. It is interesting to observe the uniform expansion.

obtained. This shows that during the implant of the modified stent the contact region would be more uniform, guaranteeing a reduced chance of tissue pinching and damage when the stent initially contacts the artery during the stent implant situation.

Accordingly, in the following we concentrate only on the modified stent design, due to its better performance during free-expansion. It is also clear that, given the stent design, it is always possible to compute local stresses and strains, verifying for deflation, *i.e.*, the final configuration.

From the simulation, we extract also some typical stenting parameters (residual stenosis, elastic recoil, foreshortening, metal/artery surface ratio) in general adopted to evaluate the stent design quality as well as short-term results. As reported in Table III, in our analyses we obtained a -6.18% residual stenosis, a 4.12% elastic recoil, a 6.97% foreshortening and 25.6% metal/artery surface ratio. The negative value for the residual stenosis indicates a light over-expansion, which

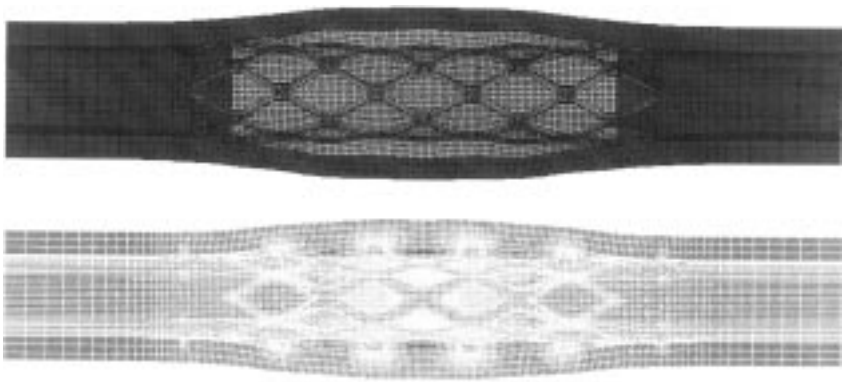

FIGURE 10 Revascularization of a stenotic artery through the insertion of a stent with modified design. Final configuration of the combined system stent + stenosis + artery and map of the contact pressures on the artery after the stent apposition.

TABLE III Stenting parameters for the original stent and the modified one

Parameters	Original stent	Modified stent
Fore-shortening	2.5% – 15%	6.97%
Metal – artery ratio	20%	25.6%
Residual stenosis	–	– 6.18%
Elastic recoil	5%	4.12%

however falls in the range ± 10% suggested in the literature [1, 6]. The remaining parameters are very close to the ones relative to the non modified J&J Palmaz – Schatz stent and available in literature, that is elastic recoil, foreshortening and metal/artery surface ratio, respectively equal to 5%, 2.5 – 15%, 20% [5, 6].

In particular, it is interesting to observe that the modified stent shows a better performance in terms of elastic recoil, especially considering that the data indicated in Table III are relative to the coupled system "stent + plaque − artery", while the data relative to the non modified J&J design are relative to a free expansion problem. This can be ascribed to the greater structural stiffness of the modified design, essentially due to the major amount of stent material (in fact, the metal/artery surface ratio is a little greater).

Finally, from the simulations, it is possible to undertake studies on the contact pressures as well as on the stresses induced in the artery by the stent apposition. Again these aspects are not discussed here for brevity.

5. CLOSURE

According to the previous discussions, the present work is directed toward a better understanding of coronary stenting bio-mechanics.

This aspect is of considerable importance since available experimental studies indicate that stent – artery mechanical interaction is one of the significative causes for the activation of restenosis mechanisms [1 – 3].

To reach this goal, we construct a three-dimensional model for studying the revascularization of a stenotic artery through the insertion of a balloon-expandable stent. In particular, the model is based on the geometrical description of an artery, plaque and a stent and for all the model components we discussed specific choices in terms of dimensions and constitutive behaviors.

We then used a commercial code (Abaqus) to perform a large-deformation analysis of the model, focusing the attention on two different stent designs and investigating their relative ability to induce an effective revascularization.

From the analyses we were able to highlight some deficiencies of the initially adopted stent

design and to propose an improved modified design. Accordingly, the paper shows the ability of accurate bio-mechanical investigations to help and improve actual methodologies.

In the future, we hope to refine the stent design and to enhance the simulation taking into account the artery composite nature and the presence of the balloon. Finally, in the longer term, we will investigate innovative auto-expandable stents made of shape memory alloys, attempting to perform a comparison with balloon-expandable systems, as well as fluid – artery interactions.

Acknowledgments

The authors would like to acknowledge dott. Francesco Versaci (Università di Roma "Tor Vergata" and European Hospital, Roma, Italy) and dott. Federico Salvi (Università di Roma "La Sapienza", Roma, Italy) for many useful discussion on the subject of the present paper.

References

[1] Freed, M., Grines, C. and Safian, R. D., *The New Manual of Interventional Cardiology*. (Physician Press, 1997).
[2] Schwartz, R. S., Huber, K. C. *et al*. (1992). *Journal of the American College of Cardiology*, **19**, 267 – 274.
[3] Trepanier, C., Leung, T. K., Tabrizian, M., Yahia, L. H., Bienvenu, J. G., Tanguay, J. F., Piron, D. L. and Bilodeau, L. (1997). *In vivo* biocompatibility study of NiTi stents. In: *Second International Conference on Shape Memory Superelastic Technologies* (Eds. Pelton, A., Hodgson, D., Russell, S. and Duerig, T.) pp. 423 – 428.
[4] Dotter, C. T. and Judkins, M. P. (1964). *Circulation*, **30**, 654.
[5] Serruys, P. and Kutryk, M. J. B., *Handbook of Coronary Stents*. (Martin Dunitz Ltd., 1998).
[6] SCIMED, Boston Scientific Corporation. *Stent Handbook*: *an educational reference guide*, 1996.
[7] Baim, D. S. (1988). *American Journal of Cardiology*, **61**.
[8] Detre, K., Holubkov, R. and Kelsey, S. (1988). *The National Heart*, *Lung and Blood Institute Registry*, *New England Journal of Medicine*, **318**, 265 – 270.
[9] Macaya, C., Serruys, P., Ruygrok, P. *et al*. (1996). *Journal of American College Cardiology*, **27**, 255 – 261.
[10] Fischman, D. L., Leon, M. B., Baim, D. S., Schatz, R. A. *et al*. (1994). *The New England Journal of Medicine*, **331**, 496 – 501.
[11] Serruys, P., de Jaegere, P., Kiemeneij, F. *et al*. (1994). *The New England Journal of Medicine*, **331**, 489 – 495.
[12] Versaci, F., Gaspardone, A., Tomai, F., Crea, F., Chiariello, L. and Gioffre, P. A. (1997). *The New England Journal of Medicine*, **336**, 817 – 822.
[13] Braunwald, E., *Heart disease*: *a textbook of cardiovascular medicine* (Saunders, W. B., 1997).
[14] Perry, M. D. and Chang, R. T. (1997). Finite element analysis of Ni – Ti alloy stent deployment. In: *Second International Conference on Shape Memory Superelastic Technologies* (Eds. Pelton, A., Hodgson, D., Russell, S. and Duerig, T.) pp. 601 – 606.
[15] Auricchio, F. and Taylor, R. L. (1997). *Computer Methods in Applied Mechanics and Engineering*, **143**, 175 – 194.
[16] Whitcher, F. D. (1997). *Computers and Structures*, **64**, 1005 – 1011.
[17] Trochu, F. and Terriault, P. (1997). Finite element stress analysis of a shape memory medical stent. In: *Second International Conference on Shape Memory Superelastic Technologies* (Eds. Pelton, A., Hodgson, D., Russell, S. and Duerig, T.) pp. 596 – 600.
[18] Trochu, F. and Terriault, P. (1998). *Computer Methods in Applied Mechanics and Engineering*, **151**, 545 – 558.
[19] Rogers, C., Tseng, D. Y., Squire, J. C. and Edelman, E. R. (1999). *Circulation Research*, **84**, 378 – 383.
[20] Andrews, S. M. *et al*. (1995). *European Journal of Endovascular Surgery*, **9**, 403 – 407.
[21] Glenn, R. *et al*. (1997). Accelerated pulsitile fatigue testing of Ni – Ti coronary stents. In: *Second International Conference on Shape Memory Superelastic Technologies* (Eds. Pelton, A., Hodgson, D., Russell, S. and Duerig, T.) pp. 585 – 590.
[22] Holzapfel, G. A., Eberlein, R., Wriggers, P. and Weizsäcker, H. W. (1996). *Computer Methods in Applied Mechanics and Engineering*, **132**, 45 – 61.
[23] Hibbit Karlsson & Sorensen, Inc. *ABAQUS*.
[24] Hayashi, K. and Yosuke, I. (1997). *Journal of Biomechanics*, **30**, 573 – 579.
[25] Born, G. V. R. and Richardson, P. D. (1990). Mechanical properties of human atherosclerotic lesions. In: *Pathophysiology of the human atherosclerotic plaque*, (Glagow, S., Newman, W. P. and Schaffa, S. A. Eds.) Springer-Verlag, pp. 413 – 423.
[26] Lendon, C. L., Davies, M. J. *et al*. (1993). *Journal of Biomedical Engineering*, **15**, 27 – 33.
[27] Lee, R. T., Grodzinsky, A. J. *et al*. (1991). *Circulation*, **83**, 1764 – 1770.
[28] Fung, Y. C., Xie, J. and Zhou, J. B. (1995). *Journal of Biomechanical Engineering*, **117**, 136 – 144.
[29] Von Maltzmann , W. W. (1984). *Journal of Biomechanics*, **17**, 839 – 847.
[30] Patel, D. J., Janicki, J. S. and Carew, T. E. (1969). *Circulation Research*, **25**, 765 – 779.
[31] Patel, D. J. and Janicki, J. S. (1970). *Circulation Research*, **27**, 149 – 158.
[32] Ogden, R. W., *Non-linear elastic deformations*. (Ellis Horwood, 1984).
[33] Fung, Y. C., *Biomechanics*: *Mechanical properties of living tissues*. (Springer-Verlag, 1993).
[34] Vaishnav, R. N., Young, J. T. and Patel, D. J. (1993). *Circulation Research*, **32**, 577 – 583.
[35] Hayashi, K. (1993). *Journal of Biomechanical Engineering*, **115**, 481 – 488.
[36] Fung, Y. C., Liu, S. Q. and Zhou, J. B. (1993). *Journal of Biomechanical Engineering*, **115**, 453 – 459.
[37] Holzapfel, G. A., Eberlein, R., Wriggers, P. and Weizsäcker, H. W. (1996). *Communication in Numerical Methods in Engineering*, **12**, 507 – 517.
[38] Holzapfel, G. A. and Weizsäcker, H. W. (1996). *Computers in Biology and Medicine*, **28**, 377 – 392.

[39] Chaboche, J. L. and Lemaitre, J., *Mechanics of Solid Materials*. (John Wiley & Sons, 1987).
[40] Simo, J. C. (1992). *Computer Methods in Applied Mechanics and Engineering*, **99**, 61 – 112.
[41] Simo, J. C. and Hughes, T. J. R., *Computational inelasticity*. (Springer-Verlag, 1998).
[42] Simo, J. C. (1999). Topics on the numerical analysis and simulation of plasticity. In: *Handbook of numerical analysis*, **III**. (eds. Ciarlet, P. G. and Lions, J. L.) Elsevier Science Publisher B.V.
[43] American Society for Metals. *Metals Handbook*.